

Analytical Tools for Characterizing Cellulose-Active Lytic Polysaccharide Monooxygenases (LPMOs)

Bjørge Westereng ¹

Jennifer S. M. Loose ¹

Gustav Vaaje-Kolstad ¹

Finn L. Aachmann ²

Morten Sørlie ¹

Vincent G. H. Eijsink ¹✉

Email Vincent.eijsink@nmbu.no

¹ Biotechnology and Food Science, Faculty of Chemistry **AQ1**, Norwegian University of Life Sciences, Ås, Norway

² Department of Biotechnology and Food Science, NOBIPOL, NTNU Norwegian University of Science and Technology, Trondheim, Norway

Abstract

Lytic polysaccharide monooxygenases are copper-dependent enzymes that perform oxidative cleavage of glycosidic bonds in cellulose and various other polysaccharides. LPMOs acting on cellulose use a reactive oxygen species to abstract a hydrogen from the C1 or C4, followed by hydroxylation of the resulting substrate radical. The resulting hydroxylated species is unstable, resulting in glycoside bond scission and formation of an oxidized new chain end. These oxidized chain ends are spontaneously hydrated at neutral pH, leading to formation of an aldonic acid or a gemdiol, respectively. LPMO activity may be characterized using a variety of analytic tools, the most common of which are high-performance anion exchange chromatography system with pulsed amperometric detection (HPAEC-PAD) and MALDI-TOF mass spectrometry (MALDI-MS). NMR may be used to increase the certainty of product identifications, in particular the site of oxidation. Kinetic studies of LPMOs have several pitfalls and to avoid these, it is important to secure copper saturation, avoid the presence of free transition metals in solution, and control the amount of reductant (i.e., electron supply to the LPMO). Further insight into LPMO properties may be obtained by determining the redox potential and by determining the affinity for copper. In some cases, substrate affinity can be assessed using isothermal titration calorimetry. These methods are described in this chapter.

Key words

Lytic polysaccharide monooxygenase
High-performance anion-exchange chromatography
MALDI-TOF mass spectrometry
Copper
Isothermal titration calorimetry

1. Introduction

1.1. A Short History of LPMOs

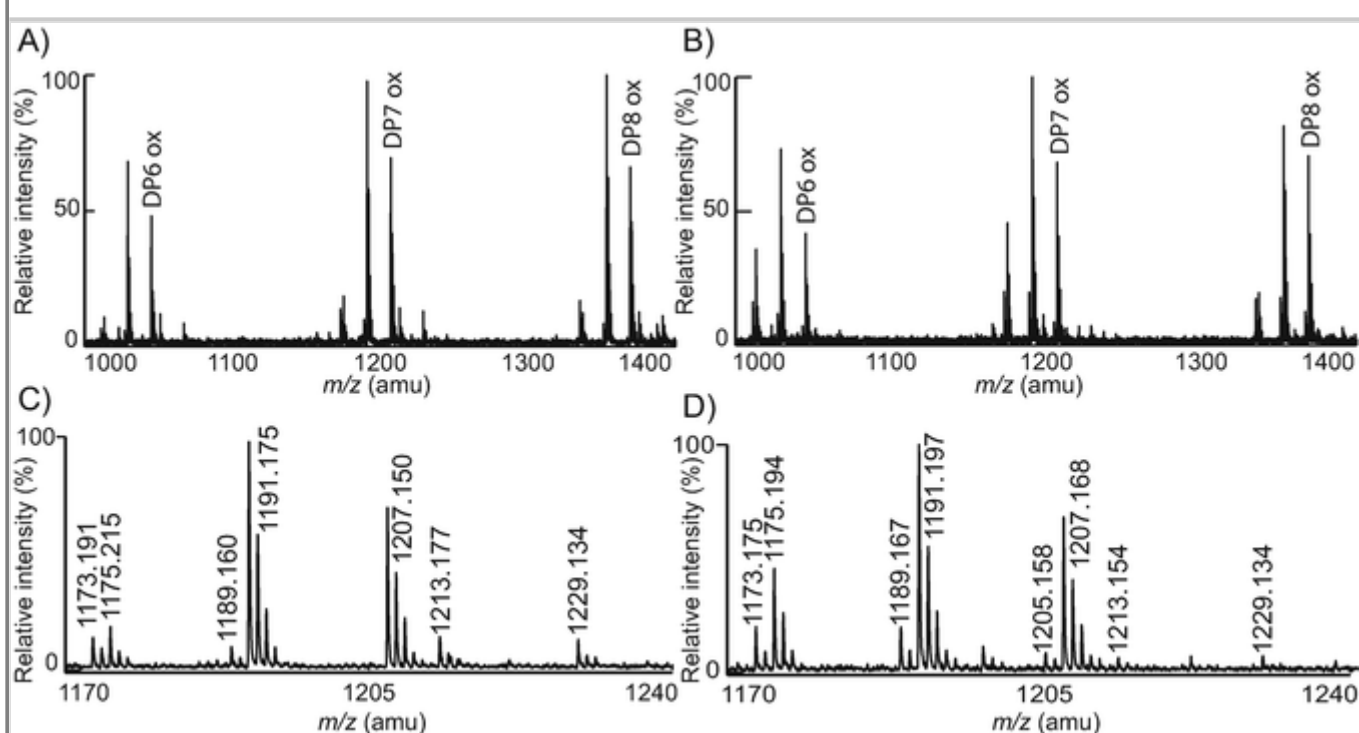
The discovery of LPMOs in 2010 by Vaaje-Kolstad et al. [1] has led to major improvements in enzymatic depolymerization of cellulose [2]. Using molecular oxygen, externally supplied electrons and a single copper ion as co-factor, LPMOs carry out oxidative cleavage of glycosidic bonds. In contrast to cellulases, which to some extent need to extract single polysaccharide chains from their crystalline context in order to productively bind their substrates, LPMOs can act directly on crystalline material [1, 3]. By introducing chain breaks, LPMOs make the crystalline substrates more accessible to the action of classical cellulases, explaining their considerable impact on the overall efficiency of the enzymatic degradation process. There is an ongoing discussion on the catalytic mechanism of these enzymes [4–6] but their products are well characterized and the nature of the expected products does not seem to depend on which catalytic mechanism is valid.

1.2. Mapping and Quantifying LPMO Activity on Cellulose

LPMOs acting on cellulose abstract a hydrogen atom from the C1 or the C4 in the scissile glycosidic bond, followed by hydroxylation of the resulting substrate-radical. The resulting hydroxylated species is unstable, resulting in glycoside bond scission and formation of an oxidized new chain end [7]. Glycosidic bond cleavage with C1 oxidation leads to formation of one chain end that is a lactone and a regular nonreducing end; the lactone is in equilibrium with the aldonic acid form, which dominates at neutral pH. Glycosidic bond cleavage with C4 oxidation leads to formation of a new regular reducing end, whereas the nonreducing end is a 4-ketosugar. The 4-keto sugar is hydrated to the corresponding gemdiol form in aqueous conditions. The lactone and the 4-keto form have identical masses and the same applies to their hydrated forms, the aldonic acid and the gemdiol. The two types of products may nevertheless be discriminated in MALDI-TOF MS because (1) the hydrated gemdiol is more easily dehydrated as a result of sample preparation for MALDI-ToF MS analysis than the aldonic acids, and (2) the aldonic acid form is charged and thus tends to form double adducts with for example sodium (Fig. 1) [8, 9].

Fig. 1

Comparison of products generated by two cellulose active LPMOs from *Thermobifida fusca*. Panels **a** and **c** show products generated by the LPMO domain of C1-oxidizing E8 (or TfLPMO10B), whereas panels **b** and **d** show products generated by C1&C4-oxidizing E7 (or TfLPMO10A). Panels **c** and **d** are zoom-in views relative to panels **a** and **b**, respectively, focusing on the heptamer cluster. The m/z values in panels **c** and **d** correspond to: 1173, sodium adduct of lactone or ketoaldose; 1175, sodium adduct of native Glc₇; 1189, potassium adduct of lactone or ketoaldose or sodium adduct of double oxidized Glc₇; 1191, sodium adduct of aldonic acid or potassium adduct of native Glc₇ or sodium adduct of gemdiol (4-ketoaldose + water); 1205, potassium adduct of double oxidized sugar; 1207, potassium adduct of aldonic acid or gemdiol form of the 1189 species; 1213, sodium adduct of the aldonic acid sodium salt; 1229, sodium adduct of the aldonic acid potassium salt. One would expect the signal at 1173 to be relatively larger in panel **d** than in panel **c**, because the 4-ketoaldose generated by C4 oxidation is less readily hydrated than the lactone generated by C1 oxidation. In the case of a C1–C4 oxidizer this is somewhat hidden because these mixed oxidizers produce more native oligomers meaning that the adjacent peak (1175) becomes stronger. The relatively higher signals at 1189 (relatively stable 4-keto form and/or sodium adduct of the double oxidized form) and at 1205 (potassium adduct of the double oxidized form) in panel **D** confirm the mixed C1 and C4-oxidizing activity of TfLPMO10A. This picture is reproduced from the supplementary information of [43]

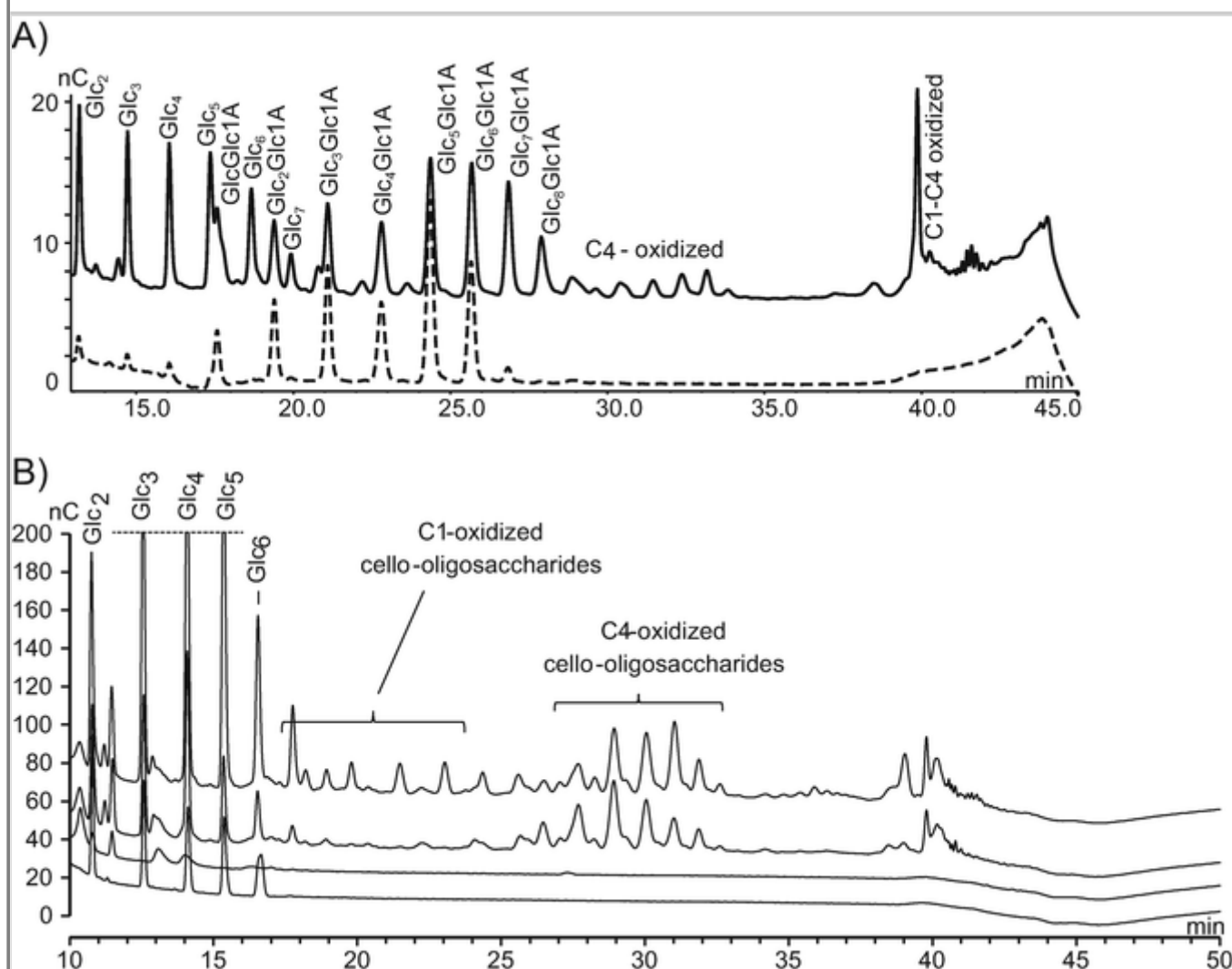


There are several chromatographic methods for analyzing the native and oxidized products, generated when an LPMO acts on cellulose [10]. The most common method, accessible in most laboratories, is high-performance anion-exchange chromatography (HPAEC) combined with pulsed amperometric detection (PAD) (Fig. 2). At the alkaline pH during the HPAEC analysis, the equilibrium between the lactone and acid is strongly shifted toward the aldonic acid, and this makes HPAEC ideal for analysis of C1-oxidized products, which are stable and negatively charged (the pK_a of cellobionic acid is 3.5 [10]), and are readily separated from native products. C4 oxidized products are less stable and undergo on-column decomposition during HPAEC [10], leading to products with additional oxidations and, importantly, native cello-oligosaccharides that have one less glucose than the original C4-oxidized product. Still, C4-oxidized products yield characteristic and diagnostic signals in HPAEC-PAD, albeit with less signal intensity due to diversion into multiple peaks and appearance later in the gradient where signal suppression by acetate becomes more prominent. Importantly, some LPMOs oxidize both C1 and C4, meaning that they have a mixed product profile that includes double-oxidized products. Products that are diagnostic for double oxidized products elute late from the column with little separation (Fig. 2; [11]) and their identity is not well resolved. A beautiful series of chromatograms, presenting many variants of product profiles is shown in Vu et al. [12].

Fig. 2

(a) HPAEC product profile for the LPMO domain of Cels2 (or *ScLPMO10C*), a bacterial C1-oxidizer (dotted chromatogram) and *ScLPMO10B*, a bacterial C1-C4 oxidizer (solid chromatogram). Native cello-oligosaccharides elute first followed by the aldonic acids. There is a slight overlap between the two product clusters, which implies that the C1-oxidized monomer and dimer elute among the late eluting native oligosaccharides. Peaks representing C4-oxidized products elute after the C1-oxidized products and tend to be lower (although this varies with the LPMO and the conditions used; for example see panel **b** and Fig. S4 in Vu et al. [12]). C4-oxidizing LPMOs tend to show higher amounts of native products (as observed here and in Fig. S4 in Vu et al. [12]), for two reasons: (1) C4-oxidized cello-oligosaccharides undergo on-column degradation reactions that lead to the formation of native cello-oligomer that are one sugar shorter than the original C4-oxidized product [10]; (2) If the LPMO can oxidize C4 and C1, as in the case of *ScLPMO10B*, its action will lead to the eventual formation of native products. The chemical identity of the compound or compounds eluting around 40 minutes in the chromatogram for the C1&C4 oxidizer only is not known, but it has been shown that peaks eluting in this area are associated with the

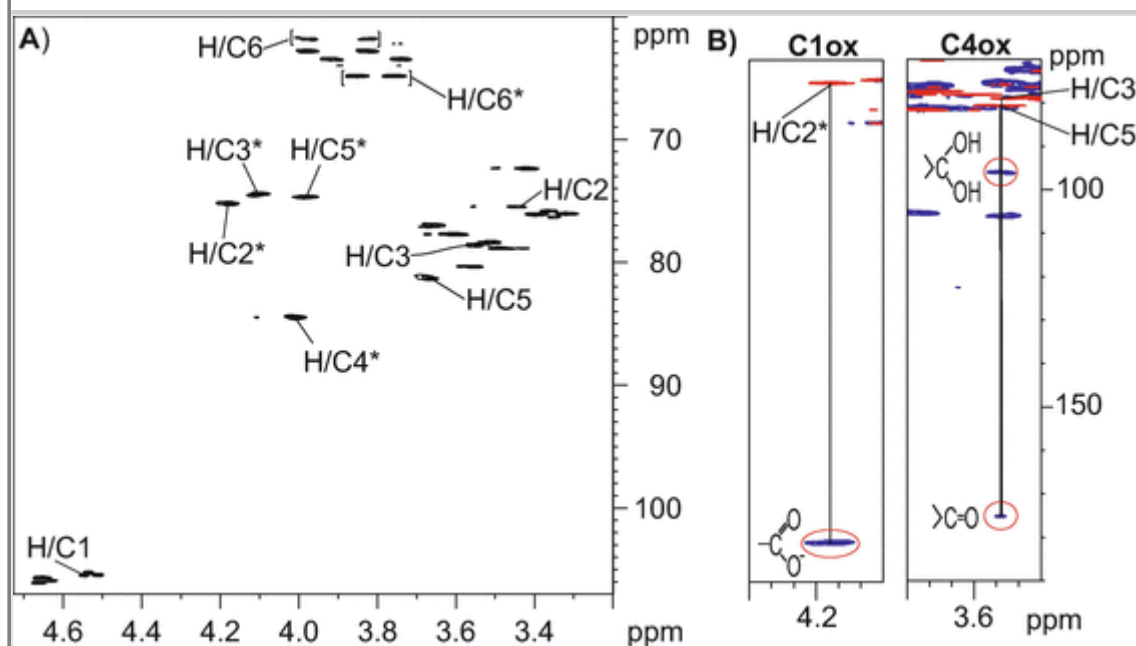
formation of double oxidized products [11]. **(b)** Products generated from cellulose by a strictly C4 oxidizing fungal LPMO, *NcLPMO9C* (upper chromatogram), and a C1&C4 oxidizing fungal LPMO, *GtLPMO9A-2* (second chromatogram from top). This panel includes chromatograms for a negative control (no enzyme) and a standard of native oligomers (lower two chromatograms). Panel **a** is reproduced from [43] and panel **b** is reproduced from [44]



Originally, there was some doubt in the field as to the nature of the oxidized products. In particular, the possibility of C6 oxidation was considered. Resolving these issues by mass spectrometry is challenging because of overlapping masses. For example, although the hydrated form of oxidized C6 is an uronic acid with an m/z difference of -2 compared with gemdiols and aldonic acids, unambiguous identification by MS is complicated by complex adduct formation patterns. Therefore, efforts have been made to use NMR for reliable product identification (Fig. 3) [11, 13]. The C1-oxidized products can be recognized by the absence of the reducing end signals (usually present at H1 α -5.22; β -4.66 ppm and C1 α -94.7; β -98.6 ppm) and more deshielded chemical shifts, especially for protons at carbons two (C2) and three (C3). On the other hand, C4-oxidized products are harder to identify as they lack signals for the proton directly attached to carbon four (C4), and show minimal changes in chemical shifts for the rest of the protons, as compared to the nonoxidized monosaccharide residues. The C1 or C4 signals (in C1 or C4-oxidized products, respectively) may be directly observed in a 1D ^{13}C NMR spectrum, but due to lack of directly attached protons they are difficult to detect. Therefore, it is recommendable to use heteronuclear multi bond correlation (HMBC), which takes advantage of heteronuclear polarization transfer, which enhances the signal by a factor of 32 and enables the detection of correlations from ^1H to ^{13}C that are mainly separated by 2 and 3 bonds (Fig. 3b).

Fig. 3

NMR analysis of the C1 and C4 oxidized LPMO products. **(a)** ^{13}C HSQC spectrum of the products generated by treating 0.9 mg/mL cellopentaose with 2.9 μM *NcLPMO9C* in the presence of 0.9 μM of cellobiose dehydrogenase (*MtCDH*). Under these conditions, the reaction will result in both C1 oxidized and C4 oxidized oligosaccharide ends. The sample was in 99.996% D_2O with 5 mM sodium acetate pD 6.0 and spectra were recorded at 25 °C. Peaks for the proton/carbon signals of the C4 oxidized monosaccharide residue are marked by H/C#, where # refers to the ring carbon number for the oxidized monosaccharide residue. Peaks for the proton/carbon signals of the C1 oxidized monosaccharide residue are marked by H/C#*. Brackets indicate pairs of proton/carbon signals attached to the same C6 (the primary alcohol group) in the oxidized monosaccharide residue. For the sake of simplicity peaks related to nonoxidized monosaccharide residues are not marked (a full assignment of chemical shifts is provided in [11]). Panel **b** shows regions of a ^{13}C HSQC spectrum overlaid by a ^{13}C HMBC spectrum recorded for products obtained in a reaction with *NcLPMO9C* and *MtCDH*. The left panel (C1ox) shows a correlation (indicated by a vertical line) from the H/C2* peak in HSQC (red) to a peak with a carbon chemical shift of 181.1 ppm in HMBC (blue), corresponding well to a carboxylate group at position C1, which is a hallmark of a C1 oxidized product. The right panel (C4ox) shows correlations from both the H/C3 and H/C5 peaks in HSQC (red) to two carbon peaks with carbon chemical shifts of 95.9 ppm and 175.2 ppm in HMBC (blue), corresponding well to the presence of a geminal diol and a keto group at C4, respectively. The signal intensity of the geminal diol is about 4 times bigger than for the keto group (approximately 80% and 20% of the signal intensity, respectively). The formed chemical groups are drawn next to the diagnostic peaks. This figure and its legend were modified from Isaksen [11]



Cellulose-active LPMOs act on a variety of cellulose substrates, such as phosphoric-acid swollen cellulose (PASC), more crystalline cellulose (Avicel) and pretreated biomass. It seems evident that LPMOs will differ in terms of their preferred substrate but systematic studies to unravel and explain such differences are lacking. For characterization purposes, PASC and Avicel are preferable substrates. Product quantification is not straightforward and opportunities and methods needed depend on the reaction setup. Reactions with commercial LPMO- and β -glucosidase-containing enzyme cocktails such as Cellic Ctec2[®] from Novozymes will yield gluconic acid and 4-keto-cellobiose only [14, 15], due to the fact that all longer oxidized products are degraded by the enzymes in the cocktail. Although this has not yet been investigated in-depth, it seems safe to assume in this case that almost all oxidized sites end up in the soluble fraction. There are several ways to quantify gluconic acid, which is stable, and for which there is a commercially available standard. Quantification of 4-keto-cellobiose is not straightforward, because there are no standards and because the

product is unstable during the HPAEC-PAD. Nevertheless, quantification has been achieved by exploiting the ability of certain C4 oxidizing LPMOs to cleave cellodextrins, thus generating two products, a C4-oxidized oligomer and an equal amount of a native oligomer, where the latter can easily be quantified [15].

Notably, when assessing the activity of LPMOs acting alone, only soluble products are usually measured and quantified. For substrates with high degrees of polymerization, such soluble products result from the LPMO cleaving twice in the same polysaccharide chain. Thus, clearly, LPMO activities will be underestimated, especially in the start of a reaction, when almost every LPMO reaction will occur in individual polymeric chains that do not become soluble upon one single cleavage. Solubilization of LPMO-generated chain ends is promoted if also cellulases are present in the reaction. Some approaches for quantification of insoluble oxidized chain ends are shortly discussed in Subheading 1.4.

AQ2

The progress of LPMO-reactions depends on many factors. The characteristics of the insoluble substrate like crystallinity, particle size, pretreatment, and the presence of lignin affect LPMO-activity. Notably, while commonly used substrate concentrations tend to seem saturating, this may not always be the case if the LPMO in question only binds to a small subfraction of the potentially heterogeneous material.

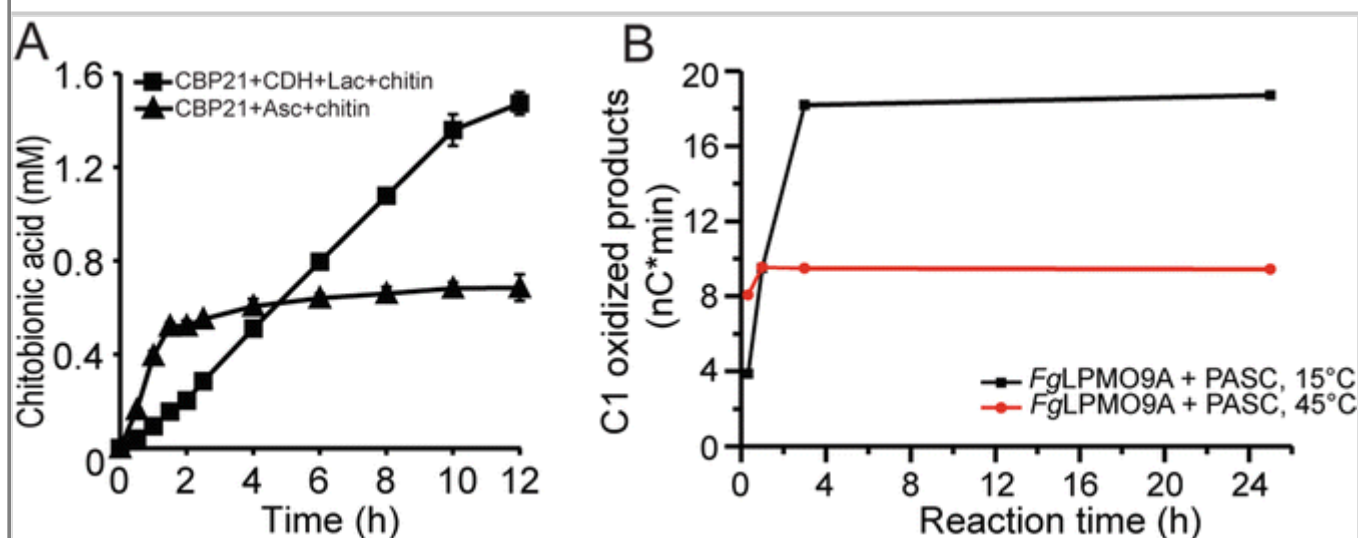
Another important factor is the choice of reductant. LPMOs are capable of using a wide array of reductants that can be either chemical reductants or another redox enzyme [1, 16–19]. The most commonly used types of reductant are small chemical reductants such as ascorbic acid, gallic acid, or reduced glutathione. The advantage of chemical reductants over the best-known protein electron donor, cellobiose dehydrogenase (CDH; [7, 20]), is that neither the cellulosic substrate nor the liberated oligosaccharides will be oxidized by the reductant. In reactions containing CDH, all soluble cellooligosaccharides will be oxidized by CDH yielding aldonic acids, i.e., products identical to products formed by C1 oxidizing LPMOs. On the other hand, it is more difficult to control chemical electron donors due to their instability in the presence of metal ions, their oxidation by the LPMO, and, often, the dependence of their redox potential on pH. Another potential complication lies in the fact that certain reductants may give interfering signals during product analysis. Furthermore, some chemical reductants may cause side reactions resulting in even more complex reaction kinetics and product mixtures. The benefit of protein electron donors is that they can be controlled and maintain electron supply stable over a long time. Moreover, it may be possible to chromatographically monitor simultaneously the activity of both the LPMO and the electron donating enzyme (e.g., [21]), which may lead to increased insight into reaction kinetics (e.g., [21]). Considering that CDH is active on cello-oligosaccharides, we expect increased use of other enzymatic electron supplying systems ([16, 22] in the near future.

Literature data show that LPMOs often display nonlinear kinetics during typical LPMO reactions (Fig. 4; [6, 21, 23], the reasons of which are often unclear, although recently, some insights have been obtained (*see ref. 6, and below*). Depletion of reductant, molecular oxygen, and productive binding sites on the substrates may all contribute to the explanation of these observations. Notably, recent data indicate that autocatalytic oxidative self-inactivation of the LPMO, brought about by an imbalance between the amount of reducing power and substrate availability [6] could be a major reason for nonlinear reaction kinetics. This recent work also indicates that H₂O₂, rather than O₂ is the preferred cosubstrate of LPMOs, shedding new light on the role of the reductant [6]. While a detailed discussion of these recent developments is beyond the scope of this review, the key point to make is that, to achieve linear kinetics, reaction conditions, including the type and concentration of the reductant need to be carefully optimized.

Fig. 4

Nonlinearity of LPMO kinetics. Panel **a** shows an experiment with a chitin-active LPMO which is fueled by either ascorbic acid or CDH/lactose. With ascorbic acid, the reaction is fast but terminates early. With CDH/lactose, the reaction is slower but the system is much more stable. It is worth noting that if single time point experiments would have been done, using the same conditions, the conclusions of a 1 h and a 10 h experiment regarding reductant efficiency would have been totally different. Panel **b** shows the activity of a fungal LPMO, FgLPMO9A on cellulose at two different temperatures. In both cases, the reactions terminate early, long before substrate is depleted. The speed of the reaction shows an expected

temperature dependency, but the outcome of a 24 h incubation would be totally dominated by stability effects. Notably, control experiments showed that the inactivation of *Fg*LPMO9A at 45 °C is not due to temperature-induced unfolding. Panel **a** is reproduced from [21], whereas panel **b** is reproduced from [23]



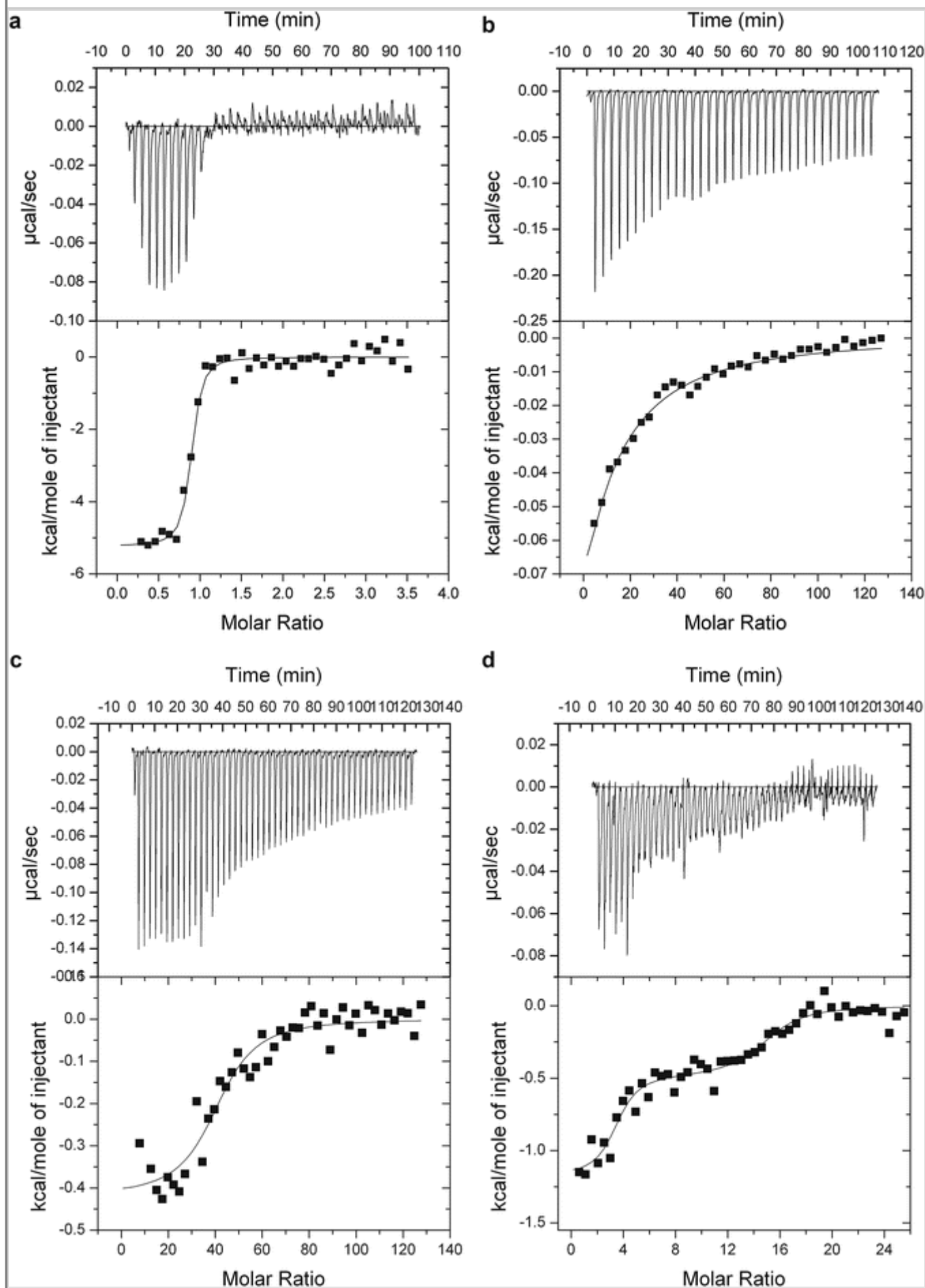
1.3. Redox Potential and the Affinity for Ligands and Co-Factor

A deeper understanding of LPMO functionalities requires insight into enzyme-substrate interactions and the chemical and electronic structure of the catalytic center. Several biophysical methods (such as EPR; e.g., [17]) and computational techniques (such as density functional theory calculation; e.g., [24]) are available to obtain such insight. Recently, the first crystal structure of an LPMO in complex with a soluble substrate has become available [25]. The pK_a values of the catalytic histidines may be determined by NMR [26].

Biochemical characterization of LPMO properties is at the basis of these advanced studies of LPMO functionality and may also help in assessing the validity of the results of computations approaches. Below, several such characterization methods are described; (1) the use of isothermal titration calorimetry for determining the affinity of the copper binding site (Fig. 5a); (2) the use of isothermal titration calorimetry for determining the affinity for the substrate (Fig. 5b–d); (3) the determination of the redox potential of the LPMO. It is worth noting that there are alternative methods for determining the redox potential [16].

Fig. 5

Thermograms (upper parts) and binding isotherms with theoretical fits (lower parts). **(a)** Binding of 150 μM of Cu^{2+} to 5 μM apo *Nc*LPMO9C at pH 5.5, 10 °C. **(b)** Binding of a 11 mM 4- β -D-cellohexaose to 30 μM of *Nc*LPMO9C at pH 5.5, 25 °C. **(c)** Binding of 500 μM of *Nc*LPMO9C- Cu^{2+} to xyloglucan from tamarind seeds (estimated at 0.9 μM), at pH 5.5, 10 °C **(d)** Binding of 500 μM of *Nc*LPMO9C- Cu^{2+} to PASC (estimated 4.5 μM) at pH 5.5, 25 °C. All data and figures are from [41], except panel A, which has not been published previously



1.4. Future Perspectives

In this chapter, we have outlined several of the methods that are currently used to characterize LPMOs. Notably, we have not addressed important biophysical methods, such as EPR and measurement of electron transfer rates. The chromatographic and mass spectrometric methods discussed shortly above have been reviewed in more detail in a previous chapter of this series [27] and in-depth discussions of the HPAEC methods and several alternatives may be found in two previous publications [10, 13]. Generally, these methods are well established, but the (in) stability of C4-oxidized products remains a challenge, which likely will be met by introducing C4-specific product modifications [28, 29].

Quantification of LPMO activity remains a challenge because of stability issues concerning both the reductant and the enzyme itself [6, 16, 21], and because it is not straightforward to monitor oxidations on the insoluble material. The stability issues must be taken very seriously to the extent that quantitative statements about LPMO activity can only be based on progress curves (and not on single time point measurements; Fig. 4a). Insight into oxidations on insoluble products may in some cases be obtained by completely solubilizing LPMO-treated material with hydrolases and then analyze soluble oxidized products (e.g., [21]). Furthermore, the use of size exclusion chromatography in ionic liquid mode for analyzing molecular distributions in cellulose [30] as well as for studying the molecular distribution of product mixtures after enzymatic treatments has a large potential to broaden our understanding of the effects of LPMO treatments. Labeling techniques are of interest, to visualize, and perhaps quantify the occurrence of oxidized chain ends in insoluble material [3, 31].

Despite their obvious importance in Nature and the biorefinery, and despite major research efforts since their discovery in 2010, several aspects of LPMOs remain enigmatic. One recent development concerns the involvement of H_2O_2 in LPMO catalysis. In particular, Bissaro et al. have shown that LPMO activity can be boosted by providing the reduced enzyme continuously with low amounts of H_2O_2 , whereas supply of higher dosages of H_2O_2 leads to rapid enzyme inactivation [6]. As noted above, quantification of LPMO activity is challenging and these recent findings may provide both an explanation and a solution to the challenge. Clearly, there is much exciting research ahead in the LPMO field. The analytical tools described below may help in further unraveling of LPMO function in nature and in the biorefinery.

2. Materials

2.1. MALDI-TOF MS

1. Equipment: Bruker Ultraflex MALDI-ToF/ToF instrument with a Nitrogen 337-nm laser beam (Bruker Daltonics GmbH, Bremen, Germany).
2. (Optional) Lithium chloride solution (the LiCl concentration should be approximately twice the concentration of the buffer used in the LPMO reaction). Dissolve the desired amount of LiCl in Milli-Q water.
3. 2,5-dihydroxybenzoic acid (DHB) solution: dissolve 4.5 mg DHB (Bruker Daltonics) in 150 μ L acetonitrile and 350 μ L water.
4. MTP 384 target plate ground steel TF from Bruker Daltonics (or equivalent).

2.2. HPAEC-PAD

1. Equipment: Ion exchange chromatography system with pulsed amperometric detection (PAD) (e.g., ICS3000, Dionex).
2. Columns: CarboPac PA1 (2 \times 250 mm) and a CarboPac PA1 guard (2 \times 50 mm) columns (Dionex, Thermo).
3. MilliQ water. Measure the desired volume of Milli-Q water (Type I, 18.2 M Ω ·cm) directly in a

dedicated HPAEC mobile phase bottle. Sonicate for 20 min to remove dissolved carbon dioxide and transfer immediately hereafter to the HPAEC system and store under N₂-saturated headspace.

4. Sodium hydroxide (0.1 M). Measure exactly 2 L of Milli-Q water (Type I, 18.2 MΩ·cm) directly in a dedicated HPAEC mobile phase bottle. Sonicate for 20 min to remove dissolved carbon dioxide and transfer immediately hereafter to the HPAEC system and store under N₂-saturated headspace. Add 10.4 mL of NaOH from a 50% (w/w) solution. Do not use NaOH pellets. Close the mobile phase bottle and swirl gently to ensure proper mixing. Maintain N₂-saturated headspace until the mobile phase is discarded.
5. Sodium acetate (1 M in 0.1 M NaOH). Dissolve 82.03 g of anhydrous sodium acetate (≥99% purity) in 1 L of Milli-Q water (Type I, 18.2 MΩ·cm). Filter the solution through no less than a 0.45 μm filter directly into a dedicated HPAEC mobile phase bottle. Sonicate for 20 min to remove dissolved carbon dioxide and transfer immediately hereafter to the HPAEC system and store under N₂-saturated headspace. Add 5.2 mL of NaOH from a 50% (w/w) solution. Do not use NaOH pellets. Close the mobile phase bottle and swirl gently to ensure proper mixing. Maintain N₂-saturated headspace until the mobile phase is discarded.

2.3. Product Identification by NMR

1. Equipment: Bruker Avance 600 MHz spectrometer equipped with a 5-mm cryogenic CP-TCI z-gradient probe.
2. High quality NMR tube 3 or 5 mm (e.g., Schott professional, Norell 509UP8, Wilmad 535-PP-7, Shigemi susceptibility matched to D₂O).
3. Deuterium oxide. 99.9% or 99.96% D₂O (Cambridge Isotope Laboratories, Andover, MA).
4. TSP stock solution (1% w/v; chemical shift reference for proton and carbon): Dissolve 0.1 g of 3-(trimethylsilyl)-propionic-2,2,3,3-d₄ acid sodium salt (Aldrich, Milwaukee, WI, USA) in 10 mL of 99.9% D₂O.
5. Buffer. Sodium acetate (5 mM, pD 6.0): Dissolve 0.041 g of anhydrous CH₃COONa in ~80 mL of H₂O, adjust the pH and hereafter adjust the volume to 100 mL with H₂O. To reduce the interference of the water signal transfer 10 mL of the acetate buffer to a 33 mm 50 mL conical centrifuge tube, lyophilize and redissolve the powder in 10 mL 99.96% D₂O.
6. Cellopentaose stock solution (0.1% w/v): Dissolve cellopentaose (1.0 mg/mL; Megazyme) in sodium acetate (5 mM, pD 6.0) and add 10 μL TSP stock solution (1‰ w/v) per mL of cellopentaose stock solution as chemical shift reference for proton and carbon.
7. Hydroquinone solution (50 mM): Dissolve 0.055 g of hydroquinone in 10 mL of 99.96% D₂O.
8. Cellobiose dehydrogenase (CDH) solution: Make an enzyme solution with a concentration of 15–20 μM CDH, e.g., CDH from *Myriococcum thermophilum* (MtCDH; [32]), using 99.96% D₂O for the dilution (*see Note 1*).
9. LPMO solution: Make an enzyme solution with a concentration of 45–60 μM LPMO using 99.96% D₂O for the dilution (*see Note 2*).
10. Oxygen gas (100%).

2.4. Copper Saturation

Copper saturation of the LPMO should be performed in the buffer that is planned used in downstream experiments and may thus vary considerably based on the experiment (for example, sodium phosphate is optimal for EPR, but incompatible with MS). Commonly used buffers are Bis-Tris pH 6.0, MES pH 6.0, sodium phosphate pH 6.0, HEPES pH 7.0 and Tris-HCl pH 8.0 in concentrations ranging from 1 to 50 mM. It should be noted that some buffers, including Tris, have the ability to bind/chelate copper and could interfere with LPMO activity, but it is so far not known whether this property of Tris influences LPMO activity under commonly used reaction conditions. However, it is advised to resaturate LPMOs with copper before experiments if they have been stored in Tris-containing buffers. A copper saturation protocol using 25 mM Bis-Tris pH 6.0 is outlined below.

1. A PD midiTrap G-25 (3.5 mL) column (GE Healthcare; *see Note 3*).
2. 25 mM BisTris buffer pH 6.0. Dissolve 0.52 g in 80 mL of Milli-Q water (Type I, 18.2 M Ω cm). Adjust to pH 6.0 with HCl and to 100 mL final volume with Milli-Q water (Type I, 18.2 M Ω cm).
3. 50 mM CuSO₄. Dissolve 0.62 g CuSO₄·5H₂O in a final volume of 50 mL Milli-Q water (Type I, 18.2 M Ω cm).

2.5. Quantitative Activity Assays

1. 2.0 mL Eppendorf tubes.
2. Substrate (e.g., Avicel or PASC) or lignin-containing substrates such as steam-exploded lignocellulosic material.
3. Buffer of choice (*see* Subheading 2.4).
4. Purified LPMO, copper-saturated as described in Subheading 3.4.
5. Cellulases, for example Cel5A from *Thermobifida fusca* or an LPMO-poor Cellulase mixture such as Celluclast (optional, if quantification of the oxidations in the soluble material or the total sample is required, respectively).
6. Reducing agent; either a small molecule reductant such as ascorbic acid or reduced glutathione (100 mM stock solution in water), gallic acid (100 mM in EtOH_{absolute}), or a protein electron donor and its substrate (e.g., cellobiose dehydrogenase and a suitable substrate, such as cellobiose or lactose).
7. Milli-Q water (Type I, 18.2 M Ω cm).
8. Thermomixer C with a thermoblock suitable for 2.0 mL tubes and a ThermoTop (Eppendorf).
9. Water bath or high-temperature heat block that can heat up to 100 °C.
10. 200 mM NaOH. Dilute 0.53 mL NaOH 50% (w/w) solution (as in Subheading 2.2) in a final volume of 50 mL Milli-Q water (Type I, 18.2 M Ω cm).
11. A MultiScreen 96-well plate filter (0.45 μ m) operated by a vacuum manifold (Millipore) and a 96-well plate.
12. Standards: native cello-oligosaccharides and cellobiose dehydrogenase, for C1-oxidized standards, or *NcLPMO9C*, for C4 oxidized standards.
13. 20 mM Tris-HCl pH 8.0. Dissolve 0.24 g Tris base in 80 mL Milli-Q water (Type I, 18.2 M Ω cm) and adjust the pH to 8.0 with HCl. Fill up to a final volume of 100 mL with Milli-Q water (Type I,

18.2 MΩ cm).

2.6. Redox Potential

1. Equipment: Ultraviolet-visible spectrophotometer (i.e., Hitachi U-1900 or Agilent Technologies Cary 8454 UV-Vis spectrophotometer). Cuvettes allowing emission at $\lambda = 610$ nm with a recommended total volume of 100 μ L to save protein solution.
2. Milli-Q water and a buffer that does not chelate copper ions (e.g., Chelex-treated 20 mM MES buffer, pH 5.5). *N,N,N',N'*-tetramethyl-1,4-phenylenediamine dihydrochloride (Sigma-Aldrich, St. Louis, MO, USA).

2.7. Measuring Affinity for Copper

1. Equipment: Isothermal titration calorimeter (e.g., a MicroCal VP-ITC, Malvern, Malvern, England).
2. A purified LPMO, Milli-Q water, a buffer that does not chelate copper ions (e.g., Chelex-treated 20 mM MES buffer, pH 5.5), and ethylenediaminetetraacetic acid (EDTA) and CuSO₄ (both form for example Sigma-Aldrich, St. Louis, MO, USA).
3. A NAP-5 column, used for desalting (GE Healthcare; *see Note 4*).

2.8. Measuring Affinity for the Substrate

1. Equipment: Isothermal titration calorimeter (e.g., a MicroCal VP-ITC, Malvern, Malvern, England).
2. A purified copper-saturated LPMO, Milli-Q water and a buffer that does not chelate copper ions (e.g., Chelex-treated 20 mM MES buffer, pH 5.5), Avicel, xyloglucan, and/or 1,4- β -D-celohexaose.

3. Methods

The protocols provided cover both common and less common methods for characterizing LPMOs. For more details, readers are directed to the original publications related to the method in question [6, 10, 11, 13, 26, 27, 33]. Where applicable, notes are appended in the Subheading 4. Additional methods, including alternative chromatographic methods, appear in another recent book in the Methods in Molecular Biology series ([27]; Subheadings 2.1, 2.2, 3.1 and 3.2, with notes adapted from this paper. For information on various electrochemical methods and EPR, the reader is referred to papers by for example the Ludwig (e.g., [16]) and Walton (e.g., [25]) groups.

3.1. MALDI-ToF MS with or Without Lithium Doping

1. To prepare samples for MALDI-ToF analysis, reactions should be run at low buffer concentrations (as a rule of thumb, less than 50 mM, preferably much less), and the use of MS-incompatible ions such as phosphate and nitrate should be avoided.
2. Centrifuge samples in an Eppendorf centrifuge at maximum speed at room temperature for 2 min.
3. Apply 2 μ L saturated DHB solution to a MALDI plate.
4. Apply 1 μ L sample, and mix with the DHB solution (on the MALDI plate).

5. Dry the spot under a stream of warm air.
6. Analyze the sample on a MALDI-ToF instrument (*see Note 3*).

Alternative method, if the mass spectrum needs simplification (*see Note 3* and [27] for details):

- (a) Mix 1 μL sample with 9 μL LiCl solution and vortex for 5 s.
- (b) Apply 2 μL saturated DHB solution to a MALDI plate. DHB is the standard matrix used for all MALDI experiments, but other matrices may work equally well.
- (c) Add 1 μL of the lithium-doped sample (point 7) to the matrix droplet on the MALDI plate.
- (d) Dry the spot under a stream of warm air.
- (e) Analyze the sample on a MALDI-ToF instrument.

3.2. HPAEC-PAD

Use an instrumental setup as described in Subheading 2.2 or similar.

1. Centrifuge samples for 3 min in an Eppendorf centrifuge at maximum speed and transfer supernatants to HPLC vials; normally no further adjustments of the samples is needed (*see Note 4*). If samples already have been filtered (*see* Subheading 3.5), this centrifugation step is not necessary.
2. Set the column temperature 30 °C and use 0.25 mL/min flow rate.
3. Use mobile phases containing 0.1 M NaOH (A) and 0.1 M NaOH, 1 M sodium acetate (B) (*see Note 5*).
4. Inject 2–10 μL sample.
5. Use the following gradient: a 10 min linear gradient from 100% A (starting condition) to 10% B, a 15 min (this step may be extended if higher resolution is needed [30] or shortened to get higher throughput) linear gradient to 30% B, a 5 min exponential gradient (Dionex curve 6) to 100% B.
6. Recondition the column by running initial conditions (100% A) for 9 min.

If there is a need for higher throughput, and if only C1-oxidations occur, a 10 min method for separation and detection of aldonic acids may be used [13]. For other applications and mass spectrometry adaptations *see* ref. 27.

3.3. Product Identification by NMR

3.3.1. NMR Sample Preparation

1. C1-oxidized products: Dissolve 0.2–2 mg of C1-oxidized product in 150 or 600 μL (for 3 or 5 mm tubes, respectively) 99.9% or 99.96% D_2O . Transfer the sample into a 3- to 5-mm high-quality NMR tube.
2. “External” method for chemical shift referencing: Insert a 3-mm NMR tube (or coaxial insert tube) into a 5-mm NMR tube with TSP (0.1‰ (w/v)) in 99.9% D_2O .
3. C4-oxidized products: Add 500 μL cellopentaose stock solution (0.1% (v/w)) to a 5 mm NMR tube

together with either 33 μL of cellobiose dehydrogenase (CDH, *MtAA3*) to a final concentration of 0.9 μM or 33 μL of hydroquinone solution (to a final concentration of 3 mM). After addition of 17 μL LPMO (e.g., *NcLPMO9C*) to a final concentration of 2.9 μM , flush the head-space of the NMR with oxygen gas (100%) for ~ 10 s before sealing the tube with parafilm around the cap. After incubation of the samples at 25 $^{\circ}\text{C}$ for 24 h, the reaction products can be analyzed by NMR spectroscopy (see **Note 1**).

3.3.2. NMR Data Acquisition and Processing

1. Set the temperature to 25 $^{\circ}\text{C}$ on the NMR spectrometer. Insert the sample in the NMR spectrometer and let the sample temperature equilibrate for ~ 10 min. After equilibration, lock on the deuterium signal and calibrate the tune, match and shims of the spectrometer according to standard operating procedures. Calibrate the ^1H and ^{13}C pulses and set spectral widths as well as other parameters in the subsequent spectra.

AQ3

2. For structural elucidation of C1- and C4-oxidized products, the following spectra can be used (the recommended pulse programs and key parameter settings are listed in brackets): 1D proton [zg30; sw 14 ppm; TD: 32 k], 2D double quantum filtered correlation spectroscopy (DQF-COSY) [cosydfphpr; TD: 2k, 512; SW 11 ppm, 11 ppm], 2D In-phase correlation spectroscopy (IP-COSY) [31] [ipcosygppr-tr; TD: 2k, 256; SW 11 ppm, 11 ppm; constant-time evolution in the indirect dimension], 2D total correlation spectroscopy (TOCSY) with 70 ms mixing time [mlevphpr; DS 128; TD: 2k, 512; SW 11 ppm, 11 ppm; d1 2 s; d9 70 ms (spin-lock mixing time)], 2D ^{13}C heteronuclear single quantum coherence (HSQC) with multiplicity editing [hsqctgppsp2.3; TD: 2k, 256; SW 11 ppm, 60 ppm, o1p 80 ppm; Cnst2 135 Hz ($^1J_{\text{CH}}$)], 2D ^{13}C HSQC- ^1H , ^1H]TOCSY with 70 ms mixing time on protons [hsqcdietgppsp2; DS 128; TD: 2k, 256; SW 11 ppm, 60 ppm, o1p 80 ppm; Cnst2 135 Hz ($^1J_{\text{CH}}$); d1 2 s (avoid RF-heating); d9 70 ms (Spin-lock mixing time)], and 2D heteronuclear multiple bond correlation (HMBC) with BIRD filter to suppress first order correlations [hsqctgpml; TD: 2k, 256; SW 11 ppm, 160 ppm, o1p 120 ppm; Cnst2 135 Hz ($^1J_{\text{CH}}$), Cnst6 125 Hz (lower filter to remove $^1J_{\text{CH}}$), Cnst7 150 Hz (higher filter to remove $^1J_{\text{CH}}$), Cnst13 8 Hz (coupling constant for long range coupling)].
3. Process and analyze the spectra using a standard NMR processing software, such as TopSpin, Mestrelab, or ACD/NMR Processor.

3.3.3. Assignment of Chemical Shifts

1. The individual monosaccharide residues are assigned by starting at the anomeric signal and/or at the primary alcohol group at C6 and then following the proton–proton connectivity using TOCSY, DQF-COSY/IP-COSY, and ^{13}C HSQC- ^1H , ^1H]TOCSY spectra. ^{13}C -HSQC is used for assigning the carbon chemical shifts. The ^{13}C HMBC spectrum provides information on connectivity between the individual monosaccharide residues as well as the chemical shifts for the oxidized carbons C1 or C4 via two-bond couplings ($^2J_{\text{CH}}$) (see **Note 6**).

3.4. Copper Saturation

1. Add a threefold molar excess of the CuSO_4 to the protein solution and incubate at room temperature for 30 min (see **Note 7**)
2. Equilibrate the PD midiTrap G-25 (3.5 mL) column (GE Healthcare) with 15 mL of the same buffer that is used in the activity assay (see **Notes 2 and 8**)
3. Add a maximum of 1.0 mL sample to the column and let it enter (see **Note 9**).

4. Elute the protein with 1.0 mL of buffer (*see Note 10*).

3.5. Quantitative Activity Assays

1. Mix the desired amount of substrate with water, buffer, and the LPMO (usually 1.0 μM). The final reaction volume should not exceed 1.5 mL.
2. Preincubate the sample at the reaction temperature for 15 min (*see Note 11*).
3. Start the reaction by adding 1.0–5.0 mM reducing agent (*see Note 12*).
4. Incubate the sample at 40 °C, shaking at ~800 rpm.
5. Collect samples in regular intervals to follow the progress of the reaction.
6. If solubilized products only are to be quantified, stop the reactions by filtration (*see Note 13*) or by boiling (note that some enzymes have are remarkably stable when substrate is present, so make sure to include proper negative controls to check for possible, however unlikely, residual activity). Filtration is preferred since this is required before analysis by HPLC to prevent particles from being injected into the system.
 - (a) If the amount of the individual oxidized oligosaccharides is to be quantified, the sample can be analyzed directly with HPAEC (Subheading 3.2). If the total amount of soluble oxidized oligosaccharides is to be quantified, add a cellulase (e.g., the GH5 endoglucanase *TfCel5A* from *T. fusca* to a final concentration of 1 μM) to the filtrates and incubate at 40 °C overnight. This will reduce the complexity of the soluble products generated by the LPMO to a mixture of glucose, cellobiose, and oxidized products with a degree of polymerization of 2 and 3 (i.e., GlcGlc1A, Glc₂Glc1A, Glc4GemGlc, and Glc4GemGlc₂), allowing quantification by HPEAC (Subheading 3.2) using the appropriate standards (*see steps 5 and 6* below for the generation of standards).
AQ4
 - (b) If only aldonic acids are formed by the LPMO, it may also be convenient to use a β -glucosidase to reduce the complexity of the product mixture (e.g., [36] added one unit of β -glucosidase from *Thermotoga maritima* (Megazyme) to 40 μL aliquots containing soluble aldonic acid cello-oligosaccharides of various DP followed by incubation for 16 h at 37 °C to obtain ~100% conversion of the products to glucose and gluconic acid).
 - (c) If insoluble oxidized sites are to be quantified, stop the reaction by boiling for 15 min and degrade the sample using a LPMO-poor cellulase cocktail under conditions that do not promote LPMO activity prior to product analysis according to Subheading 3.2 (20 mM EDTA may be added to the reaction to abolish LPMO activity, but this may give problems with downstream analysis).
7. After cellulase treatment, filter or centrifuge the samples to remove substrate remnants, before analysis by HPAEC according to Subheading 3.2.
8. A C4-oxidized standard may be prepared as described by Müller et al. [15]: Dissolve 2.5 mg of the native cello-oligosaccharide Glc₅ in 500 μL 20 mM Tris–HCl pH 8.0. Add 0.5 g/L *NcLPMO9C* (or another LPMO active on soluble cello-oligosaccharides) and 2 mM ascorbic acid and add 20 mM Tris–HCl pH 8.0 to 1.0 mL. Incubate at an appropriate reaction temperature, e.g., 33 °C for *NcLPMO9C*, for 24 h. Note that there are stability issues here (*see Notes 14 and 15*).
9. C1 oxidized standards: Dissolve an appropriate amount of native cello-oligosaccharides (e.g., 2.5 mg) in 500 μL 25 mM Bis-Tris pH 6.0 and add cellobiose dehydrogenase to a final concentration

of 2.0 μM . Incubate the sample for 48 h at 40 $^{\circ}\text{C}$ to ensure oxidation of the cellobiose (*see* **Notes 16 and 17**).

3.6. Redox Potential

1. Use an instrumental setup as described in Subheading 2.6, or similar.
2. Mix oxygen-free solutions: 50 μL 200 μM of *N,N,N',N'*-tetramethyl-1,4-phenylenediamine (TMP_{red}) in its reduced form and 50 μL , 70 μM Cu^{2+} -saturated LPMO in Chelex-treated 20 mM MES buffer pH 5.5, $t = 25$ $^{\circ}\text{C}$ in a cuvette. LPMO- Cu^{2+} solutions can be made oxygen free by sequential degassing and adding of N_2 over the solution in a stoppered vial with a rubber stopper using standard Schlenk techniques. The same approach can be used for the TMP_{red} solution. It is important that the LPMO solution is anaerobic prior to addition of TMP_{red} . An alternative method is to bubble N_2 (g) through the buffer for 1 h before the addition of TMP_{red} .
3. Determine the extent of the reaction by measuring the absorbance of the TMP radical cation (TMP_{ox}) at $\lambda = 610$ nm. Concentrations of TMP_{ox} , which equal concentrations of LPMO- Cu^{1+} , are calculated by using an extinction coefficient of 14.0/mM/cm [37].
4. This determination allows for calculations of the equilibrium concentrations for the electron transfer reaction (Eq. 1) and hence the equilibrium constant (Eq. 2).



$$K = \frac{[\text{TMP}_{\text{ox}}] [\text{LPMO-Cu}^{1+}]}{[\text{TMP}_{\text{red}}] [\text{LPMO-Cu}^{2+}]} \quad 2$$

The relationship between the free energy change (ΔG_r°), the equilibrium constant (K), and the cell potential (E°) of the reaction is shown in Eq. 3:

$$\Delta G_r^{\circ} = -RT \ln K = -nFE^{\circ} \quad 3$$

where R is the gas constant, T is the temperature in Kelvin, n is the number of electrons transferred in the reaction, and F is the Faraday constant. Summation of the measured cell potential for the equilibrium reaction (Eq. 1) with the cell potential of the $\text{TMP}_{\text{ox}}/\text{TMP}_{\text{red}}$ redox couple (273 mV vs. normal hydrogen electrode; [38]) yields the cell potential for the LPMO- $\text{Cu}^{2+}/\text{LPMO-Cu}^{1+}$ redox couple.

3.7. Measuring Affinity for Copper

1. Use an instrumental setup as described in Subheading 2.7 or similar.
2. Prepare an apo-LPMO solution by treating purified enzyme with 100 mM EDTA, followed by desalting using a NAP-5 column (GE Healthcare) equilibrated with Chelex-treated 20 mM MES buffer, pH 5.5.
3. Thoroughly degas the LPMO solution prior to experiments to avoid air bubbles in the calorimeter. The recommended concentration of apo-LPMO is 5 μM and the suggested temperature of the reaction is $t = 10$ $^{\circ}\text{C}$ (*see* **Note 18**). The volume of the LPMO solution added to the calorimeter should exceed the volume of the reaction cell. In this example, for a microcal VP-ITC with a

reaction cell volume of 1.42 mL, it is beneficial to (over)fill the reaction cell with 1.6 mL of LPMO solution.

4. Place 300 μL of 150 μM CuSO_4 in Chelex treated 20 mM MES buffer, pH 5.5 in the syringe. Inject 40 aliquots of 4 μL of the copper solution into the reaction cell, at 180 s intervals, with a stirring speed of 260 rpm. The software accompanying the calorimetric system collects ITC data automatically.
5. Prior to further analysis, correct for the heat of dilution by subtracting the heat produced by the injections of ligand into the reaction cell after completion of the binding reaction. A complementary approach is to subtract the heats produced by titrating the ligand into buffer alone in a parallel experiment. Ideally, these heats should have the same magnitude.
6. Fit data using a nonlinear least squares algorithm using a single-site binding model employed by the software that accompanies the calorimetric system to yield the stoichiometry (n), the equilibrium binding association constant (K_a), and the enthalpy change (ΔH_r°) of the reaction. The changes in reaction free energy (ΔG_r°) and entropy (ΔS_r°) as well as the dissociation constant (K_d) are calculated using the relationship in Eq. 4:

$$\Delta G_r^\circ = -RT \ln K_a = RT \ln K_d = \Delta H_r^\circ - T\Delta S_r^\circ \quad 4$$

Errors in ΔH_r° , K_d , and ΔG_r° are obtained as standard deviations of at least three experiments. Errors in ΔS_r° are obtained through propagation of errors.

7. It is worth noting that by combining the K_d for Cu^{2+} resulting from this experiment and the redox potential resulting from the method described in Subheading 3.6, one may obtain the K_d for Cu^+ , as described in detail in Fig. S2 of Aachmann et al. [26].

3.8. Measuring Affinity for the Substrate

1. Use an instrumental setup as described in Subheading 2.8 or similar.
2. For binding of small, soluble oligomers (i.e., 1,4- β -D-cellohexaose or hexa-*N*-acetyl chitohexaose), prepare a 30 μM copper-saturated LPMO solution in Chelex-treated 20 mM MES buffer, pH 5.5 (*see Note 19*).
3. Thoroughly degas the LPMO solution prior to experiments to avoid air bubbles in the calorimeter.
4. The volume of the LPMO solution added to the calorimeter should exceed the volume of the reaction cell. In this example, for a microcal VP-ITC with a reaction cell volume of 1.42 mL, it is beneficial to (over)fill the reaction cell with 1.6 mL of LPMO solution. The suggested temperature of the reaction is $t = 25^\circ\text{C}$.
5. Place 300 μL of 11 mM of the ligand in Chelex treated 20 mM MES buffer, pH 5.5 in the syringe. Inject 40 aliquots of 8 μL of the ligand solution into the reaction cell, at 180 s intervals, with a stirring speed of 260 rpm. The software accompanying the calorimetric system collects ITC data automatically.
6. Prior to further analysis, correct for the heat of dilution by subtracting the heat produced by titrating the ligand into buffer alone in a parallel experiment.
7. Fit data using a nonlinear least squares algorithm using a single-site binding model employed by the software that accompanies the calorimetric system where the stoichiometry (n) is set to be 1 (*see*

Note 19). The fitting yields the equilibrium binding association constant (K_a), and the enthalpy change (ΔH_r°) of the reaction. The changes in reaction free energy (ΔG_r°) and entropy (ΔS_r°) as well as the dissociation constant (K_d) are calculated using the relationship in Eq. 4. Errors in ΔH_r° , K_d , and ΔG_r° are obtained as standard deviations of at least three experiments. Errors in ΔS_r° are obtained through propagation of errors

8. For binding to large, soluble oligomers or insoluble polymers (i.e., xyloglucan, cellulose, chitin, etc.), place the LPMO in the syringe and the substrate in the reaction cell (*see Note 20*).
9. Prepare cellulose (phosphoric acid-swollen cellulose, PASC, 0.15 mg/mL) or xyloglucan (22 kDa, from tamarind seeds, 0.9 μ M) in Chelex-treated 20 mM MES buffer, pH 5.5 (*see Note 20*).
10. Degas and add PASC or xyloglucan in the reaction cell as described in **steps 3 and 4**. Suggested temperature of the reaction is $t = 25$ and 10 $^\circ$ C, for PASC and xyloglucan, respectively.
11. Place 300 μ L of 500 μ M of the LPMO in Chelex treated 20 mM MES buffer, pH 5.5 in the syringe. Inject 50 aliquots of 6 μ L at 180 s intervals of the ligand solution into the reaction cell with a stirring speed of 260 rpm.
12. Prior to further analysis, correct for heat of dilution by subtracting the heat produced by the injections of ligand into the reaction cell after completion of the binding reaction. A complementary approach is to subtract the heats produced by titrating the ligand into buffer alone in a parallel experiment. Ideally, these heats should have the same magnitude.
13. Fit data as described in **step 7** *without* fixing the stoichiometry (n).

4. Notes

1. The stoichiometric ratio between the LPMO and the CDH may need to be optimized for each LPMO and may also need adjustment if another CDH is used.
2. Desalting can be achieved using several standard columns and two of these appear in this paper: PD midiTrap G-25 & NAP-5, both from GE Healthcare. Note that certain carbohydrate-binding modules, which are present on some LPMOs, may bind to some of the column materials used.
3. Under standard conditions, several adducts tend to be observed during MALDI analysis (Fig. 1), the most common being sodium and potassium adducts. The fact that the m/z difference between a sodium and a potassium adduct equals the m/z difference connected to an oxygen atom complicates interpretation of mass spectra, although such interpretation is not impossible (Fig. 1). One simple way of overcoming this multiplicity of signals, which may hamper product identification, is ion doping to force the adduct composition to a defined adduct type, as described in detail in [27].
4. Samples may contain most buffers used in biochemistry labs, but avoid organic solvents (e.g., acetonitrile, methanol) in the sample matrix since several of these affect the PA-detection. Injection volumes between 2 and 10 μ L may be used. Five microliter injection has proven a suitable compromise between resolution and sensitivity. Two microliters will result in slightly improved resolution due to less sample diluent effects in HPLC. Increasing the injection volume to 10 μ L may be considered, but be aware that the sample diluent effect will affect resolution to some extent unless your sample diluent is equivalent to the eluent.
AQ5
5. When eluents are prepared, note that the 50% NaOH solution has limited use due to carbonate contamination; we usually discard these solutions when approximately half of it has been used. It is critical to follow this and other procedures for mobile phase preparation or to follow equivalent recommendations by instrument vendors, in order to achieve satisfactory results. The most important

things to pay attention to are (1) the quality of water and chemicals, (2) sufficient degassing for removal of dissolved carbon dioxide, (3) storage in an atmosphere with reduced content of carbon dioxide (N_2 or He-saturated headspace), (4) regular exchange of mobile phases (2–3 days shelf life) and (5) to avoid all kinds of detergents in mobile phases (do not use detergent washing of mobile phase bottles between eluent preparations, but restrict cleaning to rinsing with Milli-Q water, Type I, 18.2 M Ω cm). Extensive exchange of mobile phases on the column and careful column regeneration after each change of eluent are also important in order to remove accumulation of carbonate contaminations on the column.

6. 1H - ^{13}C HMBC spectra provide further insight into the nature of the products. In the HMBC spectra for the C4-oxidized products, correlations can be observed from H/C-5 and H/C-3 to a carbon chemical shift of 95.9 ppm and 175.2 ppm. These ^{13}C shifts correspond to a keto group (175.2 ppm) and its hydrated geminal diol form (95.9 ppm), and the intensity ratio between these forms depends on the pH of the sample. For the C1-oxidized products, the hydrated form (an aldonic acid) dominates; this is observed as a correlation from H/C-2 to a carbon chemical shift of 181.1 ppm.
7. The protein concentration should not exceed ~15–20 g/L. Some proteins tend to be unstable at higher concentrations when the excess of copper is added. Consider also the type of buffer that is used, since some buffers are good copper chelators.
8. Use the same buffer that is used in the activity assays. Some buffers can interfere with analytical methods. For example, MES can be detected in MALDI-TOF and HPAEC analyses.
9. It is advantageous to load lower sample volumes (~300–500 μ L) with a high concentration in order to limit dilution during desalting. Let the sample enter and add buffer to fill up the sample volume to 1.0 mL. This implies for example that one loads 400 μ L of sample followed by 600 μ L of buffer, instead of loading 1 mL of sample.
10. In order to avoid carryover of excess copper, the elution volume is reduced to 1.0 mL instead of the 1.5 mL described in the manufacturer's protocol. A second elution step using 500 μ L of buffer may be performed to collect the residual protein from the column. Note that some of the excess copper will elute in this second elution step.
11. Preincubation allows the LPMO to bind to the substrate before the reaction is started. By adding the reductant as the last component in the reaction, enzyme inactivation due to self-oxidation is prevented in the initial stage of the reaction. Enzyme inactivation is often observed, which is why it is important to always follow the progress of the reaction and to report progress curves.
12. It is important that the amount of reductant is suitable for the reaction. A good starting point is 1.0 mM of chemical reductant or 1.0 μ M cellobiose dehydrogenase and 5.0 mM lactose. It has recently been described that it is also possible to drive LPMO reactions by adding H_2O_2 [6]. In that case, H_2O_2 need to be kept low and the amount of reductant added may be substoichiometric. Regular addition of fresh H_2O_2 (and, possibly, reductant) is then necessary, since these compounds will be consumed in the course of the reaction. Too high amounts of H_2O_2 should be avoided since this may harm the enzyme. As a starting point, one may try initiating reactions by adding 10 μ M ascorbic acid and 100 μ M H_2O_2 .
13. Some LPMOs are active on soluble cello-oligosaccharides; in these cases, filtration will not stop the reaction. One may consider using ultrafiltration spin filters.
14. When using *Nc*LPMO9C under these conditions, approximately 70% of the native Glc_5 will be converted to $Glc_4gemGlc$ and Glc_3 (in equimolar amounts), whereas the rest will be un-cleaved or converted to small amounts of $Glc_4gemGlc_2$ and Glc_2 (in equimolar amounts). By quantifying the native products, the amount of C4-oxidized product in the standard sample can be determined. It is of major importance to realize that C4-oxidized sugars are unstable at high pH, which implies, among other things, that on-column degradation will occur when carrying out the chromatographic analysis described in Subheading 3.2 [10]. Thus, quantitative analysis of C4-oxidized products

according to the methods described here is not that accurate. It is obviously important to treat all samples (standard and samples from for example a progress curve) in exactly the same manner. Better quantification of C4-oxidized products may be obtained by carrying out chemical modifications prior to chromatographic analysis by HPAEC-PAD, and several methods are currently being considered and under development [28, 29]. It is also possible, albeit not straightforward, to use other chromatographic techniques, in particular PGC (Porous Graphitic Carbon chromatography) [10].

AQ6

15. Note that the procedure for producing a C4-standard described above only yields an oxidized dimer, which, consequently, is the only species that can be quantified. This is still useful since the by far dominant of C4-oxidized products obtained after incubating a cellulosic substrate with an LPMO-containing cellulase cocktail such as Cellic CTec2 is the dimeric species [15]. When using the correct chromatographic setup, the C4-oxidized dimer yields a diagnostic peak in the HPAEC chromatograms that can easily be quantified.
16. The amount of oxidized products can be determined by quantifying the nonconverted native oligomer(s) and subtracting the amounts of nonconverted oligomers from the total amount of oligomers used in the reaction. Note that CDH is active on cello-oligosaccharides of varying length and that this approach thus can be used to quantify oxidized oligomers of varying lengths.
17. The dominant C1-oxidized products obtained after incubating a cellulosic substrate with an LPMO-containing cellulase cocktail such as Cellic CTec2 are gluconic acid and cellobionic acid [14].
18. It has been observed for several LPMOs that the stoichiometry of copper ions versus LPMO is higher than 1 (i.e., 2–3) at concentrations higher than 5 μM of the protein and at reaction temperatures higher than $t = 10\text{ }^\circ\text{C}$. The origin of this behavior has not been investigated. A possible explanation is the occurrence of protein aggregation, which is more likely to take place at temperatures and protein concentrations that are higher than the concentrations that yield a 1:1 stoichiometry.
19. The shape of the ITC binding curve is described by the so-called Wiseman c value [39], which can be expressed as follows: $c = nK_a[M]_p$, where n is the stoichiometry of the reaction, K_a is the equilibrium binding association constant, and $[M]_p$ is the protein concentration. It is well established that c values within the range of $10 < c < 1000$ are a prerequisite for meaningful calculations of K_a . It has been shown, however, that binding thermodynamics can be obtained even if c is in the range of 0.01–10 if a sufficient portion of the binding isotherm is used for analysis [40]. This is achieved by ensuring a high molar ratio of ligand versus protein at the end of the titration, accurate knowledge of the concentrations of both ligand and protein, an adequate level of signal to noise in the data, and known stoichiometry. The latter implies that the value of n (i.e., 1 for a 1 to 1 binding system) needs to be fixed in the nonlinear fitting of experimental data to the theoretical model. In our experience, binding of small, soluble oligomers yields a c value below 10 [28, 39]. Figure 5a, b illustrate this concept, showing data for binding of Cu^{2+} to apo *NcLPMO9C* with a K_a of $3.0 \times 10^7\text{ M}^{-1}$ ($K_d = 33\text{ nM}$) with a c value of 150 and 1,4- β -D-cellohexaose to *NcLPMO9C*- Cu^{2+} with a K_a of $1.2 \times 10^3\text{ M}^{-1}$ ($K_d = 0.81\text{ mM}$) with a c value of 0.04. The binding isotherm changes from being sigmoidal (high c value) to hyperbolic (low c value). In the first case (Fig. 5a), the fitting can be used to determine the stoichiometry, n ; in the second case (Fig. 5b), the stoichiometry needs to be set.
20. It is in practice impossible to place insoluble polymeric substrates in the syringe in an ITC experiment, but doing so with large soluble substrates, such as xyloglucan from tamarind seeds, would in principle be possible. Still, placing PASC or the xyloglucan in the reaction cell and the LPMO in the syringe carries an advantage, since this approach allows estimation of the number of LPMO molecules binding to the substrate. In the case of *NcLPMO9C* binding to xyloglucan from tamarind seeds, an average of 30 LPMO units bind to the xyloglucan with an estimated degree of polymerization of the main chain of 594 (calculated from the sugar composition) with a K_d of $2.3\text{ }\mu\text{M}$ (Fig. 5) [41]. This suggests binding of one LPMO per 20 sugar residues in the main chain.

If the experimental setup was reversed, with the xyloglucan in the syringe and the LPMO in the reaction cell (as is the case for (Glc)₆ binding to *NcLPMO9C*), the same K_d would be observed with the reciprocal (i.e., 0.033) stoichiometry. With respect to for example PASC, the concentration of the polymer needs to be set based on an estimation of an average chain length of the polymer. As an example, Avicel-derived PASC prepared according to Zhang and Lynd is estimated to have an average chain length of 200 glucose units [42]. This Avicel-derived PASC was used in the work of Borisova et al. [41]. Here, a concentration of 4.5 μM PASC, yielding 6.4 nmol polymer chains assuming 200 glucose units per chain, was placed in the reaction cell. A total of 300 μL of a 500 μM solution of *NcLPMP9C* (150 nmol) was needed to complete LPMO binding to the PASC, and the fitting of theoretical data to the experimental data suggested that ~ 3 and ~ 11 *NcLPMO9C* bind with a K_d of 0.013 μM and 0.64 μM , respectively, per polymer chain of PASC (Fig. 5).

Acknowledgments

This work was supported by the Norwegian Research Council through grants 214613, 216162, 214138, 226244, 221576, 226247, and 244259.

References

AQ7

1. Vaaje-Kolstad G, Westereng B, Horn SJ et al (2010) An oxidative enzyme boosting the enzymatic conversion of recalcitrant polysaccharides. *Science* 330:219–222. <https://doi.org/10.1126/science.1192231>
2. Harris PV, Xu F, Kreel NE et al (2014) New enzyme insights drive advances in commercial ethanol production. *Curr Opin Chem Biol* 19:162–170. <https://doi.org/10.1016/j.cbpa.2014.02.015>
3. Eibinger M, Ganner T, Bubner P et al (2014) Cellulose surface degradation by a lytic polysaccharide monooxygenase and its effect on cellulase hydrolytic efficiency. *J Biol Chem* 289:35929–35938. <https://doi.org/10.1074/jbc.M114.602227>
4. Beeson WT, Vu VV, Span EA et al (2015) Cellulose degradation by polysaccharide monooxygenases. *Annu Rev Biochem* 84:923–946. <https://doi.org/10.1146/annurev-biochem-060614-034439>
5. Walton PH, Davies GJ (2016) On the catalytic mechanisms of lytic polysaccharide monooxygenases. *Curr Opin Chem Biol* 31:195–207. <https://doi.org/10.1016/j.cbpa.2016.04.001>
6. Bissaro B, Rohr AK, Muller G et al (2017) Oxidative cleavage of polysaccharides by monocopper enzymes depends on H₂O₂. *Nat Chem Biol Adv* 13(10):1123–1128. <https://doi.org/10.1038/nchembio.2470>. <http://www.nature.com/nchembio/journal/vaop/ncurrent/abs/nchembio.2470.html#supplementary-information>
7. Phillips CM, Beeson WT, Cate JH, Marletta MA (2011) Cellobiose dehydrogenase and a copper-dependent polysaccharide monooxygenase potentiate cellulose degradation by *Neurospora crassa*. *ACS Chem Biol* 6:1399–1406. <https://doi.org/10.1021/cb200351y>
8. Coenen GJ, Bakx EJ, Verhoef RP et al (2007) Identification of the connecting linkage between homo- or xylogalacturonan and rhamnogalacturonan type I. *Carbohydr Polym* 70:224–235
9. Westereng B, Coenen GJ, Michaelsen TE et al (2009) Release and characterization of single side chains of white cabbage pectin and their complement-fixing activity. *Mol Nutr Food Res* 53:780–789. <https://doi.org/10.1002/mnfr.200800199>
10. Westereng B, Arntzen MØ, Aachmann FL et al (2016) Simultaneous analysis of C1 and C4 oxidized oligosaccharides, the products of lytic polysaccharide monooxygenases acting on cellulose. *J*

- Chromatogr A 1445:46–54. <https://doi.org/10.1016/j.chroma.2016.03.064>
11. Isaksen T, Westereng B, Achmann FL et al (2014) A C4-oxidizing lytic polysaccharide monooxygenase cleaving both cellulose and cello-oligosaccharides. *J Biol Chem* 289:2632–2642. <https://doi.org/10.1074/jbc.M113.530196>
 12. Vu VV, Beeson WT, Phillips CM et al (2014) Determinants of regioselective hydroxylation in the fungal polysaccharide monooxygenases. *J Am Chem Soc* 136:562–565. <https://doi.org/10.1021/ja409384b>
 13. Westereng B, Agger JW, Horn SJ et al (2013) Efficient separation of oxidized cello-oligosaccharides generated by cellulose degrading lytic polysaccharide monooxygenases. *J Chromatogr A* 1271:144–152. <https://doi.org/10.1016/j.chroma.2012.11.048>
 14. Cannella D, Hsieh CW, Felby C, Jorgensen H (2012) Production and effect of aldonic acids during enzymatic hydrolysis of lignocellulose at high dry matter content. *Biotechnol Biofuels* 5:26. <https://doi.org/10.1186/1754-6834-5-26>
 15. Muller G, Varnai A, Johansen KS et al (2015) Harnessing the potential of LPMO-containing cellulase cocktails poses new demands on processing conditions. *Biotechnol Biofuels* 8:187. <https://doi.org/10.1186/S13068-015-0376-Y>
 16. Kracher D, Scheiblbrandner S, Felice AKG et al (2016) Extracellular electron transfer systems fuel cellulose oxidative degradation. *Science* 352:1098–1101. <https://doi.org/10.1126/science.aaf3165>
 17. Quinlan RJ, Sweeney MD, Lo Leggio L et al (2011) Insights into the oxidative degradation of cellulose by a copper metalloenzyme that exploits biomass components. *Proc Natl Acad Sci USA* 108(37):15079–15084. <https://doi.org/10.1073/pnas.1105776108>
 18. Westereng B, Cannella D, Agger JW et al (2015) Enzymatic cellulose oxidation is linked to lignin by long-range electron transfer. *Sci Rep* 5:18561. <https://doi.org/10.1038/srep18561>
 19. Frommhagen M, Sforza S, Westphal AH et al (2015) Discovery of the combined oxidative cleavage of plant xylan and cellulose by a new fungal polysaccharide monooxygenase. *Biotechnol Biofuels* 8:12. <https://doi.org/10.1186/s13068-015-0284-1>
 20. Langston JA, Shaghasi T, Abbate E et al (2011) Oxidoreductive cellulose depolymerization by the enzymes cellobiose dehydrogenase and glycoside hydrolase 61. *Appl Environ Microb* 77:7007–7015. <https://doi.org/10.1128/Aem.05815-11>
 21. Loose JS, Forsberg Z, Kracher D et al (2016) Activation of bacterial lytic polysaccharide monooxygenases with cellobiose dehydrogenase. *Protein Sci* 25:2175–2186. <https://doi.org/10.1002/pro.3043>
 22. Garajova S, Mathieu Y, Beccia MR et al (2016) Single-domain flavoenzymes trigger lytic polysaccharide monooxygenases for oxidative degradation of cellulose. *Sci Rep* 6:28276. <https://doi.org/10.1038/srep28276>
 23. Nekiunaite L, Petrovic DM, Westereng B et al (2016) FgLPMO9A from *Fusarium graminearum* cleaves xyloglucan independently of the backbone substitution pattern. *FEBS Lett* 590:3346–3356. <https://doi.org/10.1002/1873-3468.12385>
 24. Kim S, Ståhlberg J, Sandgren M et al (2014) Quantum mechanical calculations suggest that lytic polysaccharide monooxygenases use a copper-oxyl, oxygen-rebound mechanism. *Proc Nat Acad Sci* 111:149–154. <https://doi.org/10.1073/pnas.1316609111>

25. Frandsen KEH, Simmons TJ, Dupree P et al (2016) The molecular basis of polysaccharide cleavage by lytic polysaccharide monoxygenases. *Nat Chem Biol* 12:298. <https://doi.org/10.1038/Nchembio.2029>
26. Aachmann FL, Sorlie M, Skjak-Braek G et al (2012) NMR structure of a lytic polysaccharide monoxygenase provides insight into copper binding, protein dynamics, and substrate interactions. *Proc Natl Acad Sci USA* 109:18779–18784. <https://doi.org/10.1073/pnas.1208822109>
27. Westereng B, Arntzen MO, Agger JW et al (2017) Analyzing activities of lytic polysaccharide monoxygenases by liquid chromatography and mass spectrometry. *Methods Mol Biol* 1588:71–92. https://doi.org/10.1007/978-1-4939-6899-2_7
28. Beeson WT, Phillips CM, Cate JHD, Marletta MA (2012) Oxidative cleavage of cellulose by fungal copper-dependent polysaccharide monoxygenases. *J Am Chem Soc* 134:890–892. <https://doi.org/10.1021/Ja210657t>
29. Frommhagen M, van Erven G, Sanders M et al (2017) RP-UHPLC-UV-ESI-MS/MS analysis of LPMO generated C4-oxidized gluco-oligosaccharides after non-reductive labeling with 2-aminobenzamide. *Carbohydr Res* 448:191–199. <https://doi.org/10.1016/j.carres.2017.03.006>
30. Potthast A, Radosta S, Saake B et al (2015) Comparison testing of methods for gel permeation chromatography of cellulose: coming closer to a standard protocol. *Cellulose* 22:1591–1613. <https://doi.org/10.1007/s10570-015-0586-2>
31. Vuong TV, Liu B, Sandgren M, Master ER (2017) Microplate-based detection of lytic polysaccharide monoxygenase activity by fluorescence-labeling of insoluble oxidized products. *Biomacromolecules*. <https://doi.org/10.1021/acs.biomac.6b01790>
32. Flitsch A, Prasetyo EN, Sygmund C et al (2013) Cellulose oxidation and bleaching processes based on recombinant *Myriococcum thermophilum* cellobiose dehydrogenase. *Enzyme Microb Tech* 52:60–67. <https://doi.org/10.1016/j.enzmictec.2012.10.007>
33. Courtade G, Wimmer R, Rohr AK et al (2016) Interactions of a fungal lytic polysaccharide monoxygenase with beta-glucan substrates and cellobiose dehydrogenase. *Proc Natl Acad Sci USA* 113:5922–5927. <https://doi.org/10.1073/pnas.1602566113>
34. Forsberg Z, Vaaje-Kolstad G, Westereng B et al (2011) Cleavage of cellulose by a CBM33 protein. *Protein Sci* 20:1479–1483. <https://doi.org/10.1002/Pro.689>
35. Xia YL, Legge G, Jun KY et al (2005) IP-COSY, a totally in-phase and sensitive COSY experiment. *Magn Reson Chem* 43:372–379. <https://doi.org/10.1002/mrc.1558>
36. Gardner JG, Crouch L, Labourel A et al (2014) Systems biology defines the biological significance of redox-active proteins during cellulose degradation in an aerobic bacterium. *Mol Microbiol* 94:1121–1133. <https://doi.org/10.1111/mmi.12821>
37. Sørli M, Seefeldt LC, Parker VD (2000) Use of stopped-flow spectrophotometry to establish midpoint potentials for redox proteins. *Anal Biochem* 287:118–125. <https://doi.org/10.1006/abio.2000.4826>
38. Liu Y, Seefeldt LC, Parker VD (1997) Entropies of redox reactions between proteins and mediators: the temperature dependence of reversible electrode potentials in aqueous buffers. *Anal Biochem* 250:196–202. <https://doi.org/10.1006/abio.1997.2222>
39. Wiseman T, Williston S, Brandts JF, Lin LN (1989) Rapid measurement of binding constants and heats of binding using a new titration calorimeter. *Anal Biochem* 179:131–137. [https://doi.org/10.1016/0003-2697\(89\)90213-3](https://doi.org/10.1016/0003-2697(89)90213-3)

40. Turnbull WB, Daranas AH (2003) On the value of c : can low affinity systems be studied by isothermal titration calorimetry? *J Am Chem Soc* 125:14859–14866. <https://doi.org/10.1021/ja036166s>
41. Borisova AS, Isaksen T, Dimarogona M et al (2015) Structural and functional characterization of a lytic polysaccharide monooxygenase with broad substrate specificity. *J Biol Chem* 290:22955–22969. <https://doi.org/10.1074/jbc.M115.660183>
42. Zhang YHP, Lynd LR (2005) Determination of the number-average degree of polymerization of cellodextrins and cellulose with application to enzymatic hydrolysis. *Biomacromolecules* 6:1510–1515. <https://doi.org/10.1021/bm049235j>
43. Forsberg Z, Mackenzie AK, Sorlie M et al (2014) Structural and functional characterization of a conserved pair of bacterial cellulose-oxidizing lytic polysaccharide monooxygenases. *Proc Natl Acad Sci USA* 111:8446–8451. <https://doi.org/10.1073/pnas.1402771111>
44. Kojima Y, Varnai A, Ishida T et al (2016) Characterization of an LPMO from the brown-rot fungus *Gloeophyllum trabeum* with broad xyloglucan specificity, and its action on cellulose-xyloglucan complexes. *Appl Environ Microbiol* 82:6557–6572. <https://doi.org/10.1128/AEM.01768-16>